HHS Public Access

Author manuscript

Cancer Cell. Author manuscript; available in PMC 2016 November 09.

Published in final edited form as:

Cancer Cell. 2015 November 9; 28(5): 638–652. doi:10.1016/j.ccell.2015.09.022.

T cells engineered against a native antigen can surmount immunologic and physical barriers to treat pancreatic ductal adenocarcinoma

Ingunn M. Stromnes[1,3], **Thomas M. Schmitt**[1], **Ayaka Hulbert**[1], **J. Scott Brockenbrough**[1], **Hieu Nguyen**[1], **Carlos Cuevas**[4], **Ashley M. Dotson**[1], **Xiaoxia Tan**[3], **Jennifer L. Hotes**[1], **Philip D. Greenberg**[#1,3,5,*], and **Sunil R. Hingorani**[#1,2,5,*]

[1] Clinical Research Division, Seattle, WA, 98109

[2] Public Health Sciences Division of the Fred Hutchinson Cancer Research Center, Seattle, WA, 98109

[3] Department of Immunology, University of Washington School of Medicine, Seattle, WA, 98195

[4] Department of Radiology, University of Washington School of Medicine, Seattle, WA, 98195

[5] Division of Medical Oncology, University of Washington School of Medicine, Seattle, WA, 98195

[#] These authors contributed equally to this work.

SUMMARY

Pancreatic ductal adenocarcinomas (PDA) erect physical barriers to chemotherapy and induce multiple mechanisms of immune suppression, creating a sanctuary for unimpeded growth. We tested the ability of T cells engineered to express an affinity-enhanced T cell receptor (TCR) against a native antigen to overcome these barriers in a genetically engineered model of autochthonous PDA. Engineered T cells preferentially accumulate in PDA and induce tumor cell death and stromal remodeling. However, tumor-infiltrating T cells become progressively dysfunctional, a limitation successfully overcome by serial T cell infusions that resulted in a near-doubling of survival without overt toxicities. Similarly engineered human T cells lyse PDA cells *in vitro*, further supporting clinical advancement of this TCR-based strategy for the treatment of PDA.

[*]Correspondence: Sunil R. Hingorani, MD, PhD, Fred Hutchinson Cancer Research Center, Mail Stop M5-C800, P.O. Box 19024, Seattle, WA 98109-1024, srh@fhcrc.org, Philip D. Greenberg, MD, Fred Hutchinson Cancer Research Center, Mail Stop D3-100, P.O. Box 19024, Seattle, WA 98109-1024, pgreen@uw.edu.

AUTHOR CONTRIBUTIONS

I.M.S., T.M.S. and H.N. performed experiments. A.H., J.S.B., A.M.D., X.T. and J.L.H. generated reagents and assisted with experiments. C.C. reviewed ultrasound imaging. I.M.S., P.D.G. and S.R.H. designed the study and wrote the manuscript.

SUPPLEMENTAL INFORMATION

The Supplemental Information includes five Supplemental Figures, two Supplemental Tables and Supplemental Experimental Procedures.

Graphical Abstract

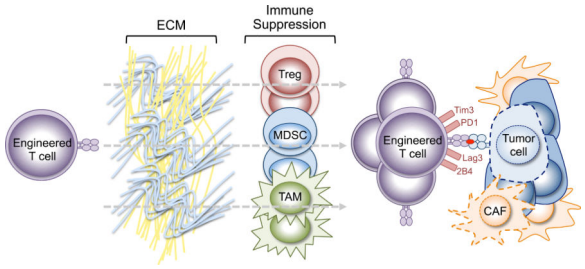

INTRODUCTION

The rising incidence and unparalleled lethality of pancreatic ductal adenocarcinoma (PDA) continue to outstrip advances in treatment (Siegel et al., 2012). Despite significant genomic instability, PDA have relatively few coding mutations compared to more immunogenic cancers (Lawrence et al., 2013). The robust desmoplastic response characteristic of PDA includes multiple mechanisms of immunosuppression that impede endogenous CD8 T cell infiltration and activity (Bayne et al., 2012; Clark et al., 2007; Feig et al., 2013; Stromnes et al., 2014a; Stromnes et al., 2014b). The limited neo-antigenic landscape together with the suppressive tumor environment likely contribute to the failure to engender effective immunity with checkpoint blockade (Brahmer et al., 2012; Le et al., 2013; Royal et al., 2010).

Pancreas cancers impose multiple constraints against immunity, including physical barriers that compromise perfusion (Jacobetz et al., 2013; Olive et al., 2009; Provenzano et al., 2012) and may also impede T cell infiltration of the tumor bed. As a result, many conventional immune strategies have had limited effect on patient survival, suggesting that targeting multiple forms of immune suppression concurrently may be necessary. Nevertheless, some clinical and preclinical data suggest it is possible to engender endogenous T cell activity, however transient. For example, vaccines designed to induce Mesothelin (MSLN)-specific T cells prolonged survival in patients with advanced PDA (Le et al., 2015), and targeted depletion of myeloid derived suppressor cells (MDSC) evoked endogenous T cell activity against autochthonous PDA (Stromnes et al., 2014a). Modulating other stromal elements in PDA may increase the therapeutic activity of more conventional immunotherapies such as checkpoint blockade (Feig et al., 2013; Winograd et al., 2015). These studies highlight both the potential and the challenges to effectively engage cancer immunity. Moreover, should an immunotherapy be sufficiently robust to alter the clinical course of a carcinoma, safety becomes a counterbalancing concern, lest autoimmunity and organ dysfunction ensue.

Mutated proteins that are obligate for tumor survival represent ideal antigens for immune targeting. Attempts to generate T cells specific for common cancer mutations in PDA, such as $KRAS^{G12D}$, have rarely proven successful, presumably due to limited processing or weak binding to HLA alleles (Chaft et al., 2014). The most reliably present and targetable cancer antigens are aberrantly expressed, non-mutated self-antigens (Argani et al., 2001). However, effectively targeting these antigens is compromised by the fact that high affinity T cells specific to self/tumor antigens undergo deletion during development, sculpting a T cell

repertoire with low affinity (Hogquist et al., 2005). To overcome this otherwise adaptive limitation in the natural repertoire, T cells can be genetically engineered with extremely high affinity against selected antigens (June et al., 2012; Stromnes et al., 2014c). Current strategies incorporate either synthetic chimeric antigen receptors (CAR) or cloned T cell receptors (TCR) and it remains to be determined which approach will be safest and best suited to treat solid malignancies (June et al., 2012; Kalos et al., 2011; Schmitt et al., 2013; Stromnes et al., 2014c).

The rigorous evaluation of the potency, safety and limitations of T cells engineered to target naturally occurring tumor antigens can be accomplished in models that faithfully recapitulate the human disease from inception to invasion. Among a panel of candidate tumor antigens that are aberrantly expressed in both human PDA and the genetically engineered $Kras^{LSL\text{-}G12D/+}$;$Trp53^{LSL\text{-}R172H/+}$;$p48^{Cre/+}$ (*KPC*) mouse model of the disease (Hingorani et al., 2003; Hingorani et al., 2005), MSLN emerged as the most attractive target. We engineered lymphocytes to express a MSLN-specific TCR with an affinity beyond that obtainable in the normal repertoire and tested their safety and ability to overcome considerable physiologic barriers to treat invasive PDA.

RESULTS

Candidate tumor antigen expression in normal tissues and murine and human PDA

To generate pure inbred *KPC* mice, each of the three requisite alleles, $Kras^{LSL\text{-}G12D}$, $Trp53^{LSL\text{-}R172H}$ and $p48^{Cre}$, were sequentially backcrossed to B6 and the progress informed by detailed SNP allelotyping. The engineered loci were the only distinguishing genetic differences in the final strains, otherwise representing 100% purity. Pure B6 *KPC* mice stochastically developed pancreatic intraepithelial neoplasms (PanIN) that spontaneously progressed to invasive and metastatic PDA, as seen with the original model on a mixed 129Sv/Bl/6 background (Hingorani et al., 2003; Hingorani et al., 2005). The histopathology of the primary tumors revealed the glandular architecture expected of an adenocarcinoma, together with an abundant inflammatory infiltrate, dense ECM, and scattered compressed blood vessels, hallmarks of human PDA and the original *KPC* model (Figure 1A and see below). B6 *KPC* mice also developed liver, lung and diaphragm metastases characterized by a complex stromal response (Figure S1A).

To inform the rational design of a T cell therapy, we first performed specific immunohistochemistry to assess a variety of potential antigenic targets overexpressed by both murine and human tumor epithelial cells in preinvasive, invasive and metastatic PDA (Figure 1A). Marked intra- and inter-tumoral heterogeneity in both preinvasive and invasive disease was observed across a number of antigens that are immunological targets in PDA including the Wilms' tumor antigen (WT1) (Koido et al., 2014; Oji et al., 2004), MUC1 (Shindo et al., 2014) and Annexin A2 (ANXA2) (Zheng and Jaffee, 2012). WT1 was absent from normal pancreas and expressed primarily in stromal cells of preinvasive and invasive PDA. MUC1 was expressed in normal pancreas and PanIN and was heterogeneous in PDA and metastases. ANXA2 was expressed at low levels in normal pancreatic ducts and to a higher degree in PanIN, PDA and metastases. Other antigens, such as COX2, are either highly expressed in tumor cells as well as normal tissues, precluding safe immunological

targeting; or, as with EGFR and Her2/Neu, are expressed more heterogeneously (Hingorani et al., 2005). In comparison, despite some variation in intensity, MSLN was reliably expressed in all preinvasive, invasive and metastatic PDA specimens examined (Figure 1A). MSLN staining also identified micrometastases (Figure S1B). MSLN-expressing cells were positive for cytokeratin (CK) (Figure 1B), consistent with a ductal phenotype, and negative for the activated fibroblast marker, αSMA (Figure S1C). $MSLN^+$ cells in PDA were positive for *Trp53* (Figures 1C and S1C), reflecting expression of stabilized point-mutant *Trp53*, and also expressed low levels of MHC class I which was induced by IFNγ (not shown), as seen in studies of human PDA (Pandha et al., 2007). MSLN mRNA isolated from primary tumor epithelial cells was highly expressed (comparable to the ductal marker CK19) and significantly higher than WT1 (Figure 1D), consistent with the immunohistochemical analyses.

Despite being expressed in some normal tissues (Chang and Pastan, 1996), mice that lack MSLN have no discernable phenotype (Bera and Pastan, 2000) revealing that it is not essential for life. We detected MSLN in the normal pleura and pericardium, as well as in rare cells in the thymus, raising the possibility of central and peripheral tolerance to this self-antigen (Figures S1D-S1F). Human and murine MSLN share 55% amino acid identity and have similar expression profiles in normal tissues (Bera and Pastan, 2000; Chang and Pastan, 1996). There are also no known species differences in the regulation or function of MSLN. In summary, the absence of detectable MSLN in normal pancreas, increase in expression with disease progression (Figure 1E), high expression in invasive PDA and metastases and the suggestion that MSLN may promote tumor invasion (Chen et al., 2013) all contribute to its attractiveness as an immune target (see also Pastan and Hassan, 2014).

Generation and safety of affinity-enhanced TCR cell therapy

We immunized B6 $MSLN^{-/-}$ and wild-type (WT) mice with a recombinant adenovirus expressing murine MSLN (Ad-MSLN) to elicit reactive T cells. T cells specific for epitopes $MSLN_{343\text{-}351}$, $MSLN_{484\text{-}492}$, $MSLN_{544\text{-}552}$ and $MSLN_{583\text{-}591}$ were isolated from $MSLN^{-/-}$ mice but not WT mice, consistent with central tolerance (Figure 2A). However, both $MSLN^{-/-}$ and WT mice generated responses to $MSLN_{406\text{-}414}$, previously shown to be processed and presented by a B6 ovarian cancer cell line (Hung et al., 2007). $MSLN_{406\text{-}414}$-specific T cells isolated from WT mice uniformly expressed the Vβ9 TCR chain as did the majority of $MSLN_{406\text{-}414}$-specific T cells from $MSLN^{-/-}$ mice (Figures S2A). Despite expressing similar levels of Vβ9, $MSLN_{406\text{-}414}$-specific T cell lines from $MSLN^{-/-}$ mice stained brighter with tetramer, consistent with higher affinity (Figures S2A and S2B). $MSLN^{-/-}$ $MSLN_{406\text{-}414}$-specific T cell clones also responded to lower antigen concentrations than the corresponding WT clones (Figure S2C). We therefore focused on the isolation and study of these $MSLN_{406\text{-}414}$ T cells as the murine surrogate for the potential isolation and subsequent genetic modification of a naturally occurring human TCR for clinical applications (June et al., 2012; Schmitt et al., 2009; Stromnes et al., 2014c).

Most T cell clones isolated from WT and $MSLN^{-/-}$ mice used the same germline Vα4 and Vβ9 TCR chains, restricting any sequence differences between the highest affinity from the respective strains to CDR3 (Figure 2B), the region that directly contacts peptides (Jorgensen

et al., 1992; Kelly et al., 1993). These results suggest a similar preferential docking geometry of TCR chains for recognition of this epitope. We inserted codon-optimized TCR chains into retroviral vectors for expression in transgenic P14 T cells that endogenously express a TCR specific for the LCMV gp33 epitope (Pircher et al., 1989). As expected, T cells expressing the highest affinity TCR isolated from MSLN$^{-/-}$ mice (TCR_{1045}) stained brighter with tetramer and responded to 10-fold lower antigen concentration than the highest affinity cells (TCR_{7431}) from WT mice (Figures 2C and 2D). Tetramer decay kinetics confirmed the higher affinity of TCR_{1045} (Figure 2E).

The contribution of CD8 binding to MHC class I on target cells or tetramers can minimize differences in TCR affinities for peptide in MHC complexes (Daniels and Jameson, 2000; Denkberg et al., 2001; Garcia et al., 1996). To better assess affinity differences, we transduced the CD8$^-$ 58 TCR$\alpha\beta^{-/-}$ cell line (Letourneur and Malissen, 1989) with CD8α and β and expressed TCR_{7431} or TCR_{1045} in both CD8$^+$ and CD8$^-$ cells. TCR_{1045} bound tetramer independently of CD8, whereas TCR_{7431} binding required CD8 (Figure 2F), suggesting TCR_{1045} might also be useful in CD4$^+$ T cells. TCR_{1045} T cells lysed *KPC* MHC class I$^+$ tumor cells more effectively than TCR_{7431} T cells (Figures 2G-2I). TCR_{1045} therefore represents an “affinity-enhanced” TCR and models what may be achieved by engineering CDR3 to optimize human TCR (Schmitt et al., 2009).

The value of an affinity-enhanced TCR depends upon improved function without prohibitive toxicity. Extensive experiments were performed to verify the safety and activity of engineered T cells in mice. Adoptively transferred TCR_{1045} T cells were detected in normal tissues at low frequency (≤1% of CD45$^+$ cells) and did not express activation markers (Figures S2D and S2E). Conditioning with cyclophosphamide, but not gemcitabine, increased the expansion and memory formation of engineered T cells (Figures S2F-S2I), perhaps reflecting a more complete depletion of endogenous immune cells (data not shown). Persisting donor T cells expanded and downregulated CD62L following vaccination (Figure S2J). Basal levels of MSLN expression in normal organs did not elicit self-reactivity even in the context of vaccine- and lymphopenia-induced activation/expansion and IL-2 administration (Figure S2K), as reflected by lack of infiltration, accumulation or tissue injury.

Tumor-specific accumulation, activity and suppression of TCR_{1045} engineered T cells

We transduced P14 T cells with either TCR_{1045} or a control TCR (TCR_{gag}) specific to a retrovirus gag epitope (Dossett et al., 2009) to formally assess activity. After two *in vitro* stimulations, transduced T cells uniformly exhibited an effector phenotype (Figure S3A). *In vitro*-expanded T cells also transiently expressed inhibitory receptors PD1, Tim3, and 2B4, which reflect activation but can be associated with dysfunction. However, the transduced T cells secreted IFNγ after antigen encounter (Figure 2D) and were therefore clearly functional, suggesting that the post-stimulation receptor profile reflected a transient response from TCR signaling rather than T cell exhaustion.

A series of pilot studies was performed to evaluate the *in vivo* efficacy of this therapy in *KPC* mice with a defined pancreatic tumor. Donor TCR_{1045} cells were detected in the lungs at 2 hr post transfusion (presumably in vascular capillary beds) and redistributed to the

pancreas by 4 days (Figure 3A). Preferential accumulation in pancreatic tumors of TCR_{1045}- versus TCR_{gag}-transduced T cells was observed (Figure 3B). Similar percentages and numbers of donor T cells were detected in the spleen irrespective of TCR specificity, whereas the frequency and number of intratumoral TCR_{1045} T cells were significantly higher than that of TCR_{gag} T cells (Figures 3C and 3D). TCR_{1045} T cells were distributed throughout the tumor bed, interspersed within the stroma as well as adjacent to epithelial cells (Figure 3E). $Trp53^{+}CK^{-}$ cells in the stroma could be found in close contact with TCR_{1045} cells (Figure 3F) and may reflect tumor cells that had undergone EMT: CK^{+} cells in glandular structures co-expressed the prototypic epithelial marker E-cadherin but $Trp53^{+}CK^{-}$ cells in the stroma did not (Figure S3B). As expected, $Trp53^{+}CK^{-}$ cells also did not express the myeloid marker, CD11b, or the endothelial marker, CD31 (Figures S3C and S3D).

Increased tumor cell apoptosis was observed 8 days following TCR_{1045} T cell infusion, but not at day 28, indicative of a specific, albeit transient anti-tumor effect (Figures 3G and 3H). TCR_{1045} T cells also caused marked stromal involution (Figures 3I and 3J), as seen after anti-CD40 administration (Beatty et al., 2011) or targeted depletion of myeloid cells (Stromnes et al., 2014a). The failure to sustain target cell apoptosis suggested that the donor T cells either did not persist in the tumor and/or lost function. At day 28, TCR_{1045} cells were rare in the spleen, thymus, bone marrow, blood, salivary gland and draining lymph node (dLN), yet remained enriched in PDA (Figures 4A and 4B, and not shown). Nevertheless, TCR_{1045} T cell numbers decreased ~6-fold in spleen but ~18-fold in PDA between 8 and 28 days (Figure 4C), revealing a selective disadvantage for T cell survival in the tumor and consistent with the short-lived fate of differentiated effector T cells (Berger et al., 2008; Kaech et al., 2003). Intratumoral and splenic TCR_{1045} T cells bound tetramer with similar affinity, indicating the tumor does not modulate TCR expression (Figure 4D). In contrast to either splenic TCR_{1045} or intratumoral TCR_{gag} cells, intratumoral TCR_{1045} cells expressed Ki67, CD25, 41BB and CD69, revealing TCR signaling from specific antigen recognition (Figures 4E and 4F). In contrast, down-regulation of CD27, CXCR3 and CD44 on intratumoral donor T cells was independent of antigen specificity (Figures 4E, 4F, S4A and S4B). Intratumoral TCR_{1045} cells also progressively and selectively upregulated PD1, Tim3, Lag3, and 2B4, which were not expressed on splenic TCR_{1045} cells (Figures 4G and 4H) or intratumoral TCR_{gag} cells (Figure S4B), and such $PD1^{high}$ cells can be refractory to PD-L1 blockade (Blackburn et al., 2009).

A significantly lower fraction of intratumoral versus splenic TCR_{1045} T cells secreted IFNγ and TNFα in response to antigen (Figures 4I and 4J), consistent with chronic TCR signaling and subsequent inhibitory receptor expression. However, non-specific TCR_{gag} T cells isolated from tumors also had decreased function compared to their splenic counterparts (Figures 4I and 4J) revealing that T cell dysfunction in PDA is also, in part, independent of these inhibitory receptors and persistent TCR signaling. $CD4^{+}Foxp3^{+}$ regulatory T cells (Treg), myeloid-derived suppressor cells (MDSC) and numerous suppressive factors are enriched in PDA (Figures S4C and S4D) and may contribute to T cell suppression in the tumor microenvironment independent of TCR signaling.

A second infusion of TCR_{1045} engineered cells readily infiltrates PDA

We next examined whether PDA remain susceptible to a second infusion of TCR_{1045} cells, providing a ready clinical strategy to circumvent the observed loss of function over time. The serial infusions were distinguished by injecting $Thy1.2^+/1.2^+$ *KPC* hosts first with $Thy1.1^+/1.2^+$ TCR_{1045} T cells and infusing $Thy1.1^+/1.1^+$ TCR_{1045} T cells 20 days later (Figures 5A and 5B). The 2nd infusion also preferentially accumulated in PDA compared to other tissues (Figures 5C and 5D). At 8 days after transfer, the 2nd infusion of cells expressed less PD1, Tim3, and Lag3 in PDA and dLN compared to cells persisting from the 1st infusion (Figure 5C and data not shown). The 2nd infusion increased the total number of PDA-localized donor T cells 10-fold (data not shown) and they were also more functional after 8 days than cells persisting from the 1st infusion in the same tumor (day 28) (Figure 5E).

Serial T cell infusions promote the survival of mice with advanced PDA

Encouraged by the pilot studies, we conducted a randomized, blinded, placebo-controlled trial with overall survival (OS) as the primary endpoint in *KPC* mice with invasive PDA (Table S1). Secondary endpoints included objective response and tumor cell apoptosis. Mice were enrolled based on a defined tumor burden and randomized to receive either engineered TCR_{1045} or TCR_{gag} T cell infusions every 2 weeks. The majority (63%) of *KPC* mice receiving TCR_{1045} cells showed objective responses. In contrast, all of the TCR_{gag} cell recipients imaged serially showed progressive disease (Figures 6A and 6B). At necropsy, TCR_{1045}-recipient mice had noticeably hemorrhagic tumors (Figure 6C); an influx of mononuclear cells and loss of collagen were also observed, even in regions deep within the tumor bed (Figures 6C and S5A). Intratumoral vascular density was similar between control and TCR_{1045} cohorts, indicating that T cell therapy did not induce angiogenesis (Figures 6C and S5B). However, TCR_{1045} cell therapy did significantly increase vessel patency (Figure 6D). Prolonged T cell therapy did not induce detectable pleural or pericardial pathology (Figure S5C) and the number of donor T cells, endogenous $CD8^+$ T cells and myeloid cells in these locations were also similar between the two cohorts (Figure S5D-F), underscoring the safety profile of this approach.

The intensity of MSLN expression in primary PDA decreased in the majority (6/10) of TCR_{1045} cell recipients evaluated but remained high in all (6/6) TCR_{gag} recipients examined, consistent with selection for tumor cell variants expressing lower levels of target antigen (Figures 6E and 6F). Regions of marked tumor epithelial cell apoptosis in TCR_{1045} T cell recipients were also observed (Figures 6G and 6H) and a higher frequency of intratumoral TCR_{1045} cells expressed activation markers 41BB, CD69 and Ki67 (Figure 6I and data not shown). In comparison, we did not detect significant differences in myeloid ($CD11b^+$) or endothelial ($CD31^+$) cell apoptosis between the cohorts (Figure S5G). Endothelial cells were rare, however, in areas of high tumor cell apoptosis in TCR_{1045} recipients (Figure S5H) and their loss may have been secondary to tumor destruction. A modest but significant increase in apoptosis of αSMA^+ fibroblasts was detected in TCR_{1045} cell recipients (Figures S5I and S5J), which may contribute to the decreased collagen content. Since αSMA^+ fibroblasts do not appear to express MSLN (Figure S1C), the stromal

cell apoptosis could reflect ligation of death receptors, loss of paracrine signaling from tumor epithelial cells, or MSLN uptake and cross-presentation.

A significant and preferential increase in intratumoral TCR_{1045} vs. TCR_{gag} cell frequency was observed compared to the spleen (Figure S5K). Fewer tumor-infiltrating TCR_{1045} cells persisted after the final infusion than after the first infusion (data not shown), but only the first infusion was preceded by lymphodepletion and this difference could reflect the absence of induced cytokines that promote T cell proliferation and survival.

Trends toward decreased numbers of animals with metastatic disease (64% in TCR_{gag} vs. 46% in TCR_{1045} cohort) and malignant ascites (43% vs. 15%) were also observed (Table S1), consistent with the observed specific TCR_{1045} cell infiltration into metastases, expression of markers induced by antigen recognition and increased apoptosis (Figures S5L-S5N). Median OS from time of enrollment nearly doubled from 54 days for TCR_{gag} recipients to 96 days for the TCR_{1045} T cell group (Figure 6J), on par with or exceeding previous therapies tested in *KPC* mice, all of which depended on cytotoxic chemotherapy (Olive et al., 2009; Provenzano et al., 2012; Winograd et al., 2015). Thus, we demonstrate an effective T cell based therapy for invasive PDA that is safe and also circumvents the need for non-specific and toxic chemotherapy or radiotherapy.

Cloning and evaluation of human MSLN-reactive TCR

Appropriate target epitope selection is critical for the successful translation of T cell therapy (Chapuis et al., 2013; Stromnes et al., 2014c). To isolate receptors for patient treatment, we attempted to expand human MSLN-reactive T cells from normal donors to several peptides previously identified as HLA-A1 and HLA-A2 restricted epitopes (Table S2). We were able to generate T cell lines from two previously described, dominant HLA-A2-restricted epitopes, $MSLN_{20-28}$ and $MSLN_{530-538}$ (Thomas et al., 2004). $MSLN_{20-28}$ and $MSLN_{530-538}$-specific T cells are associated with improved outcomes in vaccinated PDA patients (Le et al., 2015; Thomas et al., 2004) suggesting that these epitopes are endogenously processed and presented and that the corresponding T cells have therapeutic activity. We cloned these T cells and measured tetramer binding (Figure 7A). The highest affinity $MSLN_{20-28}$-specific T cell clone had ~10-fold increased sensitivity to antigen compared to the highest affinity $MSLN_{530-538}$-specific clone (Figure 7B). The TCR that stained brightest with tetramer and had the highest functional avidity were cloned, sequenced, codon-optimized, inserted into lentiviral vectors and expressed in human T cells. The $MSLN_{20-28}$-specific TCR bound tetramer independently of CD8 whereas $MSLN_{530-538}$-specific TCR required CD8 (Figure 7C). The $MSLN_{20-28}$ and the $MSLN_{530-538}$ TCR were also expressed in primary human CD8 T cells, indicating successful competition with the endogenous TCR for expression (Figure 7D). The human Panc-1 PDA cell line expresses both MSLN (Figure 7E) and HLA-A2, and the latter could be increased by IFNγ (Figure 7F). Human CD8 T cells transduced to express either the $MSLN_{20-28}$- or $MSLN_{530-538}$-specific TCR specifically lysed HLA-$A2^+$ $MSLN^+$ Panc-1 cells, confirming their ability to recognize endogenously processed and presented antigen and kill tumor cells (Figure 7G). These receptors provide the essential substrate for genetic modifications of the CDR3

domains to produce an affinity enhanced TCR and translate our findings to patients with $MSLN^+$ malignancies.

DISCUSSION

The relative paucity of endogenous CD8 T cells in PDA has been attributed to the presence of immunosuppressive cells (Clark et al., 2007; Feig et al., 2013; Stromnes et al., 2014a) and elevated interstitial pressures. We show here that affinity-enhanced TCR T cells can nevertheless effectively infiltrate PDA, modify the ECM, induce tumor cell death and significantly prolong the survival of *KPC* mice with established invasive disease. The preferential accumulation of engineered TCR_{1045} cells in PDA indicates that energy-dependent T cell trafficking can overcome biophysical barriers to the passive transport of small molecules (Jacobetz et al., 2013; Provenzano et al., 2012) and overcome immunosuppression sufficiently to kill tumor cells. T cell-mediated tumor rejection has largely been studied with transplantable tumor models or artificially overexpressed antigens; however, such systems may not accurately reflect the breadth of obstacles to clinical translation, as evidenced by SV40-driven models of gastric and prostate cancer in which adoptively transferred T cells induced regression of engrafted tumors but not of the equivalent autochthonous disease (Bourquin et al., 2010; Chou et al., 2012). In a retrovirally-induced, *Kras*-driven lung cancer model engineered to overexpress ovalbumin, endogenous (naïve) ovalbumin-specific T cells delayed cancer progression but resistant tumors emerged that had lost the model antigen, highlighting a problem with artificially introduced antigens (DuPage et al., 2011). Thus, previous studies in transplantable or autochthonous solid tumor models have not adequately illuminated how to incorporate effector T cells specific to naturally expressed self/tumor antigens.

The adoptive T cell therapy described here can provide sustained clinical benefit and animals were treated for months without apparent on- or off-target toxicities. Unlike targeted ablation of stromal fibroblasts in autochthonous PDA which appeared to unleash a more aggressive disease (Ozdemir et al., 2014; Rhim et al., 2014), the T cell therapy presented here remodeled the stroma, including death of fibroblasts, and still conferred a survival benefit. Enzymatic degradation of hyaluronan in combination with gemcitabine also significantly increased survival in *KPC* mice and was accompanied by the loss of both tumor epithelial cells and activated fibroblasts (Provenzano et al., 2012). Thus, stromal remodeling in certain contexts can be beneficial.

T cell-mediated remodeling of the matrix was antigen-dependent, raising the question of which cell type(s) present MSLN to donor T cells in PDA. The increased apoptosis of fibroblasts with TCR_{1045} T cells suggests that MSLN may be cross-presented by stromal cells (Qin and Blankenstein, 2000; Spiotto et al., 2004; Zhang, 2008). Alternatively, direct lysis of tumor epithelial cells could have resulted in the loss of critical paracrine factors that promote stromal cell survival and/or function, indirectly decreasing collagen content. Understanding the precise mechanisms of antigen recognition and cell destruction in PDA has clinical implications, particularly as MSLN is abundantly shed from the cell surface (Pastan and Hassan, 2014) and could be taken up by neighboring cells. In this regard, a TCR-based therapy may have an advantage over MSLN-targeting CAR currently in clinical

trials (Beatty et al., 2014), as the latter would not recognize cross-presented antigen and might also be inhibited by shed soluble antigen. A greater understanding of stromal contributions to anti-tumor T cell activity will undoubtedly inform future studies and refinements of this strategy.

Engineered T cells became progressively dysfunctional in PDA and upregulated the inhibitory receptors PD1, Lag3, Tim3 and 2B4, reflecting chronic TCR signaling. They did not express detectable levels of Foxp3, a transcriptional factor expressed in Treg, either prior to transfer or after PDA infiltration (data not shown). Since the majority of the $PD1^+$ T cells co-expressed additional inhibitory receptors, determining if blockade of any of these pathways alone or in concert increases intratumoral T cell function is a cogent next step. We note that control TCR_{gag} T cells recovered from tumors also exhibited dysfunction. Thus, a component of the observed diminished T cell activity was independent of antigen recognition and the inhibitory receptor profile, highlighting a separate contributing role of the immunosuppressive TME. Together with the limited neo-antigen landscape in PDA (Lawrence et al., 2013), these results may help explain why PD1/PDL1 pathway blockade has not been effective in PDA patients, despite showing marked results against some malignancies (Brahmer et al., 2012; Topalian et al., 2012). Maximizing engineered T cell activity may require overcoming inhibitory pathways downstream of persistent TCR signaling as well as relieving the generalized immunosuppression that is independent of TCR specificity.

That affinity-enhanced TCR therapy selects for tumor cells expressing lower levels of MSLN highlights both the selective pressure that can be achieved with such an approach and a potential limitation of targeting only a single antigen. That T cells nevertheless continued to be activated in tumors despite decreased MSLN expression also emphasizes the potential value of a high affinity TCR. Our murine data reveal that many epitopes within MSLN are poorly immunogenic, emphasizing the importance of epitope selection when targeting antigens. The $MSLN_{20\text{-}28}$ and $MSLN_{530\text{-}538}$ epitopes are both immunogenic in humans and can elicit T cells that are associated with increased survival in PDA patients. The human $MSLN_{20\text{-}28}$-specific TCR we describe here also binds tetramer avidly and independently of CD8 and therefore represents an excellent starting point for initial trials. Understanding how to further refine TCR engineering to be more effective and how best to combine engineered T cells with agents that modulate the TME, including strategies to increase antigen presentation, may greatly expand their therapeutic potential. Targeting additional tumor antigens may also prove valuable for achieving more complete and durable responses. Nevertheless, the results reported here, including objective response and increased survival with T cells alone – and in an autochthonous model that may be incurable due to inherently multifocal disease and continual regeneration of new tumors – strongly support efforts to begin translating genetically engineered TCR-based cell therapy targeting known human tumor antigens to patients with PDA and other solid tumors.

EXPERIMENTAL PROCEDURES

Mouse Strains

The Institutional Animal Care and Use Committees of the Fred Hutchinson Cancer Research Center and the University of Washington approved all animal studies. *Kras* $^{LSL\text{-}G12D/+}$*;Trp53* $^{LSL\text{-}R172H/+}$*;p48* ^{Cre} *(KPC)* mice have been previously described (Hingorani et al., 2005). To place the alleles on a pure defined background, each strain was independently serially back-crossed to C57Bl/6 H-2^{b} genetic background informed by SNP allelotyping (RADIL, IDEXX-Bioresearch). Final enrichment of the B6 genetic backgrounds was assessed at 1449 genomic SNPs using GoldenGate Genotyping Assays (Illumina, Inc.) at the DartMouse Speed Congenic Core Facility (Dartmouth Medical School). Raw SNP data were analyzed with SNaP-MAP™ and Map-Synth™ software. Both female and male mice were included. MSLN$^{-/-}$ mice were generously provided by Ira Pastan (NCI, Bethesda, MD) and previously described (Bera and Pastan, 2000). P14 mice have been previously described (Pircher et al., 1989).

Human specimens

All studies using human specimens were approved by the Fred Hutchinson Cancer Research Center Institutional Review Board and conducted according to the principles expressed in the Declaration of Helsinki. Tumor tissues were obtained from patients who provided written informed consent by NWBioTrust (Department of Pathology, University of Washington, Seattle, WA).

Cloning mouse MSLN$_{406\text{-}414}$-specific TCR and generation of plasmids

The Vα4 and Vβ9 TCR chains from the highest affinity wild-type and MSLN$^{-/-}$ T cell clones were cloned using RACE PCR, codon optimized (Invitrogen), linked by a porcine teschovirus-1 2A element and inserted into the Mig-R1 retroviral vector, as previously described (Schmitt et al., 2013).

Statistics

The Kolmogorov-Smirnov test was used to test whether data met the assumption of normality. The Students' t test was used to compare normally distributed two-group data. Multigroup data were analyzed using 2-way ANOVA followed by a Tukey post test to correct for multiple comparisons. All data are shown as mean ± SEM unless otherwise indicated. A Fisher's exact test was used to compare the difference in the frequency of events (e.g. metastases, ascites). Kaplan-Meier survival data were analyzed using a Log-rank (Mantel-Cox) Test. Unless otherwise indicated, symbols indicate statistical significance as follows: *, $p<0.05$; **, $p<0.005$; ***, $p<0.0005$.

Supplementary Material

Refer to Web version on PubMed Central for supplementary material.

ACKNOWLEDGEMENTS

We thank Markus Carlson, Yen Ho, Fiona Pakiam, Joseph Ryan, Natalie Duerkopp, Megan Larmore and the University of Washington histology core for technical support. We are grateful to Shelley Thorsen, Nathan Lee and Deborah Banker for assistance with manuscript and figure preparation. We thank Howard Crawford for generously providing partially back-crossed $p48^{Cre/+}$ mice. This work was supported by Fred Hutchinson Cancer Research Center/University of Washington Cancer Consortium Cancer Center Support Grant CA015704 (S.R.H. and P.D.G.), Giles W. and Elise G. Mead Foundation (S.R.H.), Safeway Foundation (S.R.H.), a gift from Maryanne Tagney and David Jones (S.R.H.), National Institutes of Health National Cancer Institute (CA18029 and CA33084 to P.D.G.; CA161112 to S.R.H.), and grants from the Korean Research Institute of Bioscience and Biotechnology (P.D.G.), Juno Therapeutics (P.D.G.) and the Irvington Institute Fellowship Program of the Cancer Research Institute and the Jack and Sylvia Paul Estate Fund to Support Collaborative Immunotherapy Research (I.M.S). P.D.G. has ownership interest (including patents) in and is a consultant/advisory board member for Juno Therapeutics. The content is solely the responsibility of the authors and does not necessarily represent the official views of the National Institutes of Health.

REFERENCES

Argani P, Iacobuzio-Donahue C, Ryu B, Rosty C, Goggins M, Wilentz RE, Murugesan SR, Leach SD, Jaffee E, Yeo CJ, et al. Mesothelin is overexpressed in the vast majority of ductal adenocarcinomas of the pancreas: identification of a new pancreatic cancer marker by serial analysis of gene expression (SAGE). Clin Cancer Res. 2001; 7:3862–3868. [PubMed: 11751476]

Bayne LJ, Beatty GL, Jhala N, Clark CE, Rhim AD, Stanger BZ, Vonderheide RH. Tumor-derived granulocyte-macrophage colony-stimulating factor regulates myeloid inflammation and T cell immunity in pancreatic cancer. Cancer Cell. 2012; 21:822–835. [PubMed: 22698406]

Beatty GL, Chiorean EG, Fishman MP, Saboury B, Teitelbaum UR, Sun W, Huhn RD, Song W, Li D, Sharp LL, et al. CD40 agonists alter tumor stroma and show efficacy against pancreatic carcinoma in mice and humans. Science. 2011; 331:1612–1616. [PubMed: 21436454]

Beatty GL, Haas AR, Maus MV, Torigian DA, Soulen MC, Plesa G, Chew A, Zhao Y, Levine BL, Albelda SM, et al. Mesothelin-specific chimeric antigen receptor mRNA-engineered T cells induce anti-tumor activity in solid malignancies. Cancer immunology research. 2014; 2:112–120. [PubMed: 24579088]

Bera TK, Pastan I. Mesothelin is not required for normal mouse development or reproduction. Mol Cell Biol. 2000; 20:2902–2906. [PubMed: 10733593]

Berger C, Jensen M, Lansdorp P, Gough M, Elliott C, Riddell S. Adoptive transfer of effector CD8+ T cells derived from central memory cells establishes persistent T cell memory in primates. J Clin Invest. 2008; 118:294–305. [PubMed: 18060041]

Blackburn SD, Shin H, Haining WN, Zou T, Workman CJ, Polley A, Betts MR, Freeman GJ, Vignali DA, Wherry EJ. Coregulation of CD8+ T cell exhaustion by multiple inhibitory receptors during chronic viral infection. Nat Immunol. 2009; 10:29–37. [PubMed: 19043418]

Bourquin C, von der Borch P, Zoglmeier C, Anz D, Sandholzer N, Suhartha N, Wurzenberger C, Denzel A, Kammerer R, Zimmermann W, Endres S. Efficient eradication of subcutaneous but not of autochthonous gastric tumors by adoptive T cell transfer in an SV40 T antigen mouse model. J Immunol. 2010; 185:2580–2588. [PubMed: 20644173]

Brahmer JR, Tykodi SS, Chow LQ, Hwu WJ, Topalian SL, Hwu P, Drake CG, Camacho LH, Kauh J, Odunsi K, et al. Safety and activity of anti-PD-L1 antibody in patients with advanced cancer. N Engl J Med. 2012; 366:2455–2465. [PubMed: 22658128]

Chaft JE, Litvak A, Arcila ME, Patel P, D'Angelo SP, Krug LM, Rusch V, Mattson A, Coeshott C, Park B, et al. Phase II study of the GI-4000 KRAS vaccine after curative therapy in patients with stage I-III lung adenocarcinoma harboring a KRAS G12C, G12D, or G12V mutation. Clin Lung Cancer. 2014; 15:405–410. [PubMed: 25044103]

Chang K, Pastan I. Molecular cloning of mesothelin, a differentiation antigen present on mesothelium, mesotheliomas, and ovarian cancers. Proc Natl Acad Sci U S A. 1996; 93:136–140. [PubMed: 8552591]

Chapuis AG, Ragnarsson GB, Nguyen HN, Chaney CN, Pufnock JS, Schmitt TM, Duerkopp N, Roberts IM, Pogosov GL, Ho WY, et al. Transferred WT1-Reactive CD8+ T Cells Can Mediate Antileukemic Activity and Persist in Post-Transplant Patients. Sci Transl Med. 2013; 5:174ra127.

Chen SH, Hung WC, Wang P, Paul C, Konstantopoulos K. Mesothelin binding to CA125/MUC16 promotes pancreatic cancer cell motility and invasion via MMP-7 activation. Sci Rep. 2013; 3:1870. [PubMed: 23694968]

Chou CK, Schietinger A, Liggitt HD, Tan X, Funk S, Freeman GJ, Ratliff TL, Greenberg NM, Greenberg PD. Cell-intrinsic abrogation of TGF-beta signaling delays but does not prevent dysfunction of self/tumor-specific CD8 T cells in a murine model of autochthonous prostate cancer. J Immunol. 2012; 189:3936–3946. [PubMed: 22984076]

Clark CE, Hingorani SR, Mick R, Combs C, Tuveson DA, Vonderheide RH. Dynamics of the immune reaction to pancreatic cancer from inception to invasion. Cancer Res. 2007; 67:9518–9527. [PubMed: 17909062]

Daniels MA, Jameson SC. Critical role for CD8 in T cell receptor binding and activation by peptide/major histocompatibility complex multimers. J Exp Med. 2000; 191:335–346. [PubMed: 10637277]

Denkberg G, Cohen CJ, Reiter Y. Critical role for CD8 in binding of MHC tetramers to TCR: CD8 antibodies block specific binding of human tumor-specific MHC-peptide tetramers to TCR. J Immunol. 2001; 167:270–276. [PubMed: 11418659]

Dossett ML, Teague RM, Schmitt TM, Tan X, Cooper LJ, Pinzon C, Greenberg PD. Adoptive Immunotherapy of Disseminated Leukemia With TCR-transduced, CD8(+) T Cells Expressing a Known Endogenous TCR. Mol Ther. 2009; 17:742–749. [PubMed: 19209146]

DuPage M, Cheung AF, Mazumdar C, Winslow MM, Bronson R, Schmidt LM, Crowley D, Chen J, Jacks T. Endogenous T cell responses to antigens expressed in lung adenocarcinomas delay malignant tumor progression. Cancer Cell. 2011; 19:72–85. [PubMed: 21251614]

Feig C, Jones JO, Kraman M, Wells RJ, Deonarine A, Chan DS, Connell CM, Roberts EW, Zhao Q, Caballero OL, et al. Targeting CXCL12 from FAP-expressing carcinoma-associated fibroblasts synergizes with anti-PD-L1 immunotherapy in pancreatic cancer. Proc Natl Acad Sci U S A. 2013; 110:20212–20217. [PubMed: 24277834]

Garcia KC, Scott CA, Brunmark A, Carbone FR, Peterson PA, Wilson IA, Teyton L. CD8 enhances formation of stable T-cell receptor/MHC class I molecule complexes. Nature. 1996; 384:577–581. [PubMed: 8955273]

Hingorani SR, Petricoin EF, Maitra A, Rajapakse V, King C, Jacobetz MA, Ross S, Conrads TP, Veenstra TD, Hitt BA, et al. Preinvasive and invasive ductal pancreatic cancer and its early detection in the mouse. Cancer Cell. 2003; 4:437–450. [PubMed: 14706336]

Hingorani SR, Wang L, Multani AS, Combs C, Deramaudt TB, Hruban RH, Rustgi AK, Chang S, Tuveson DA. Trp53R172H and KrasG12D cooperate to promote chromosomal instability and widely metastatic pancreatic ductal adenocarcinoma in mice. Cancer Cell. 2005; 7:469–483. [PubMed: 15894267]

Hogquist KA, Baldwin TA, Jameson SC. Central tolerance: learning self-control in the thymus. Nat Rev Immunol. 2005; 5:772–782. [PubMed: 16200080]

Hung CF, Tsai YC, He L, Wu TC. Control of mesothelin-expressing ovarian cancer using adoptive transfer of mesothelin peptide-specific CD8+ T cells. Gene Ther. 2007; 14:921–929. [PubMed: 17377599]

Jacobetz MA, Chan DS, Neesse A, Bapiro TE, Cook N, Frese KK, Feig C, Nakagawa T, Caldwell ME, Zecchini HI, et al. Hyaluronan impairs vascular function and drug delivery in a mouse model of pancreatic cancer. Gut. 2013; 62:112–120. [PubMed: 22466618]

Jorgensen JL, Esser U, Fazekas de St Groth B, Reay PA, Davis MM. Mapping T-cell receptor-peptide contacts by variant peptide immunization of single-chain transgenics. Nature. 1992; 355:224–230. [PubMed: 1309938]

June C, Rosenberg SA, Sadelain M, Weber JS. T-cell therapy at the threshold. Nat Biotechnol. 2012; 30:611–614. [PubMed: 22781680]

Kaech SM, Tan JT, Wherry EJ, Konieczny BT, Surh CD, Ahmed R. Selective expression of the interleukin 7 receptor identifies effector CD8 T cells that give rise to long-lived memory cells. Nat Immunol. 2003; 4:1191–1198. [PubMed: 14625547]

Kalos M, Levine BL, Porter DL, Katz S, Grupp SA, Bagg A, June CH. T cells with chimeric antigen receptors have potent antitumor effects and can establish memory in patients with advanced leukemia. Sci Transl Med. 2011; 3:95ra73.

Kelly JM, Sterry SJ, Cose S, Turner SJ, Fecondo J, Rodda S, Fink PJ, Carbone FR. Identification of conserved T cell receptor CDR3 residues contacting known exposed peptide side chains from a major histocompatibility complex class I-bound determinant. Eur J Immunol. 1993; 23:3318–3326. [PubMed: 8258346]

Koido S, Homma S, Okamoto M, Takakura K, Mori M, Yoshizaki S, Tsukinaga S, Odahara S, Koyama S, Imazu H, et al. Treatment with chemotherapy and dendritic cells pulsed with multiple Wilms' tumor 1 (WT1)-specific MHC class I/II-restricted epitopes for pancreatic cancer. Clin Cancer Res. 2014; 20:4228–4239. [PubMed: 25056373]

Lawrence MS, Stojanov P, Polak P, Kryukov GV, Cibulskis K, Sivachenko A, Carter SL, Stewart C, Mermel CH, Roberts SA, et al. Mutational heterogeneity in cancer and the search for new cancer-associated genes. Nature. 2013; 499:214–218. [PubMed: 23770567]

Le DT, Lutz E, Uram JN, Sugar EA, Onners B, Solt S, Zheng L, Diaz LA Jr. Donehower RC, Jaffee EM, Laheru DA. Evaluation of Ipilimumab in Combination With Allogeneic Pancreatic Tumor Cells Transfected With a GM-CSF Gene in Previously Treated Pancreatic Cancer. J Immunother. 2013; 36:382–389. [PubMed: 23924790]

Le DT, Wang-Gillam A, Picozzi V, Greten TF, Crocenzi T, Springett G, Morse M, Zeh H, Cohen D, Fine RL, et al. Safety and survival with GVAX pancreas prime and Listeria Monocytogenes-expressing mesothelin (CRS-207) boost vaccines for metastatic pancreatic cancer. J Clin Oncol. 2015; 33:1325–1333. [PubMed: 25584002]

Letourneur F, Malissen B. Derivation of a T cell hybridoma variant deprived of functional T cell receptor alpha and beta chain transcripts reveals a nonfunctional alpha-mRNA of BW5147 origin. Eur J Immunol. 1989; 19:2269–2274. [PubMed: 2558022]

Oji Y, Nakamori S, Fujikawa M, Nakatsuka S, Yokota A, Tatsumi N, Abeno S, Ikeba A, Takashima S, Tsujie M, et al. Overexpression of the Wilms' tumor gene WT1 in pancreatic ductal adenocarcinoma. Cancer Sci. 2004; 95:583–587. [PubMed: 15245594]

Olive KP, Jacobetz MA, Davidson CJ, Gopinathan A, McIntyre D, Honess D, Madhu B, Goldgraben MA, Caldwell ME, Allard D, et al. Inhibition of Hedgehog signaling enhances delivery of chemotherapy in a mouse model of pancreatic cancer. Science. 2009; 324:1457–1461. [PubMed: 19460966]

Ozdemir BC, Pentcheva-Hoang T, Carstens JL, Zheng X, Wu CC, Simpson TR, Laklai H, Sugimoto H, Kahlert C, Novitskiy SV, et al. Depletion of carcinoma-associated fibroblasts and fibrosis induces immunosuppression and accelerates pancreas cancer with reduced survival. Cancer Cell. 2014; 25:719–734. [PubMed: 24856586]

Pandha H, Rigg A, John J, Lemoine N. Loss of expression of antigen-presenting molecules in human pancreatic cancer and pancreatic cancer cell lines. Clin Exp Immunol. 2007; 148:127–135. [PubMed: 17302733]

Pastan I, Hassan R. Discovery of mesothelin and exploiting it as a target for immunotherapy. Cancer Res. 2014; 74:2907–2912. [PubMed: 24824231]

Pircher H, Burki K, Lang R, Hengartner H, Zinkernagel RM. Tolerance induction in double specific T-cell receptor transgenic mice varies with antigen. Nature. 1989; 342:559–561. [PubMed: 2573841]

Provenzano PP, Cuevas C, Chang AE, Goel VK, Von Hoff DD, Hingorani SR. Enzymatic targeting of the stroma ablates physical barriers to treatment of pancreatic ductal adenocarcinoma. Cancer Cell. 2012; 21:418–429. [PubMed: 22439937]

Qin Z, Blankenstein T. CD4+ T cell--mediated tumor rejection involves inhibition of angiogenesis that is dependent on IFN gamma receptor expression by nonhematopoietic cells. Immunity. 2000; 12:677–686. [PubMed: 10894167]

Rhim AD, Oberstein PE, Thomas DH, Mirek ET, Palermo CF, Sastra SA, Dekleva EN, Saunders T, Becerra CP, Tattersall IW, et al. Stromal elements act to restrain, rather than support, pancreatic ductal adenocarcinoma. Cancer Cell. 2014; 25:735–747. [PubMed: 24856585]

Royal RE, Levy C, Turner K, Mathur A, Hughes M, Kammula US, Sherry RM, Topalian SL, Yang JC, Lowy I, Rosenberg SA. Phase 2 trial of single agent Ipilimumab (anti-CTLA-4) for locally advanced or metastatic pancreatic adenocarcinoma. J Immunother. 2010; 33:828–833. [PubMed: 20842054]

Schmitt TM, Aggen DH, Stromnes IM, Dossett ML, Richman SA, Kranz DM, Greenberg PD. Enhanced-affinity murine T-cell receptors for tumor/self-antigens can be safe in gene therapy despite surpassing the threshold for thymic selection. Blood. 2013; 122:348–356. [PubMed: 23673862]

Schmitt TM, Ragnarsson GB, Greenberg PD. T cell receptor gene therapy for cancer. Hum Gene Ther. 2009; 20:1240–1248. [PubMed: 19702439]

Shindo Y, Hazama S, Maeda Y, Matsui H, Iida M, Suzuki N, Yoshimura K, Ueno T, Yoshino S, Sakai K, et al. Adoptive immunotherapy with MUC1-mRNA transfected dendritic cells and cytotoxic lymphocytes plus gemcitabine for unresectable pancreatic cancer. J Transl Med. 2014; 12:175. [PubMed: 24947606]

Siegel R, Naishadham D, Jemal A. Cancer statistics, 2012. CA Cancer J Clin. 2012; 62:10–29. [PubMed: 22237781]

Spiotto MT, Rowley DA, Schreiber H. Bystander elimination of antigen loss variants in established tumors. Nat Med. 2004; 10:294–298. [PubMed: 14981514]

Stromnes IM, Brockenbrough JS, Izeradjene K, Carlson MA, Cuevas C, Simmons RM, Greenberg PD, Hingorani SR. Targeted depletion of an MDSC subset unmasks pancreatic ductal adenocarcinoma to adaptive immunity. Gut. 2014a; 63:1769–1781. [PubMed: 24555999]

Stromnes IM, Greenberg PD, Hingorani SR. Molecular pathways: myeloid complicity in cancer. Clin Cancer Res. 2014b; 20:5157–5170. [PubMed: 25047706]

Stromnes IM, Schmitt TM, Chapuis AG, Hingorani SR, Greenberg PD. Re-adapting T cells for cancer therapy: from mouse models to clinical trials. Immunol Rev. 2014c; 257:145–164. [PubMed: 24329795]

Thomas AM, Santarsiero LM, Lutz ER, Armstrong TD, Chen YC, Huang LQ, Laheru DA, Goggins M, Hruban RH, Jaffee EM. Mesothelin-specific CD8(+) T cell responses provide evidence of in vivo cross-priming by antigen-presenting cells in vaccinated pancreatic cancer patients. J Exp Med. 2004; 200:297–306. [PubMed: 15289501]

Topalian SL, Hodi FS, Brahmer JR, Gettinger SN, Smith DC, McDermott DF, Powderly JD, Carvajal RD, Sosman JA, Atkins MB, et al. Safety, activity, and immune correlates of anti-PD-1 antibody in cancer. N Engl J Med. 2012; 366:2443–2454. [PubMed: 22658127]

Winograd R, Byrne KT, Evans RA, Odorizzi PM, Meyer AR, Bajor DL, Clendenin C, Stanger BZ, Furth EE, Wherry EJ, Vonderheide RH. Induction of T cell immunity overcomes complete resistance to PD-1 and CTLA-4 blockade and improves survival in pancreatic carcinoma. Cancer immunology research. 2015

Zhang B. Targeting the stroma by T cells to limit tumor growth. Cancer Res. 2008; 68:9570–9573. [PubMed: 19047130]

Zheng L, Jaffee EM. Annexin A2 is a new antigenic target for pancreatic cancer immunotherapy. Oncoimmunology. 2012; 1:112–114. [PubMed: 22720228]

SIGNIFICANCE

Immune therapies hold considerable promise for the treatment of cancer. Although notable successes have been achieved in hematologic malignancies, progress in solid tumors has been more elusive. Pancreatic ductal adenocarcinomas present an especially formidable challenge given the robust desmoplasia that accompanies disease progression, creating barriers to both drug perfusion and anti-tumor immunity. We show here that T cells engineered to express affinity-enhanced T cell receptors reactive to Mesothelin, a native tumor antigen, can transiently overcome both the inordinately elevated interstitial pressures and the multiple modes of immune suppression to specifically infiltrate PDA and induce tumor cell death. Serial adoptive transfers of such engineered T cells can be given safely and significantly increase overall survival.

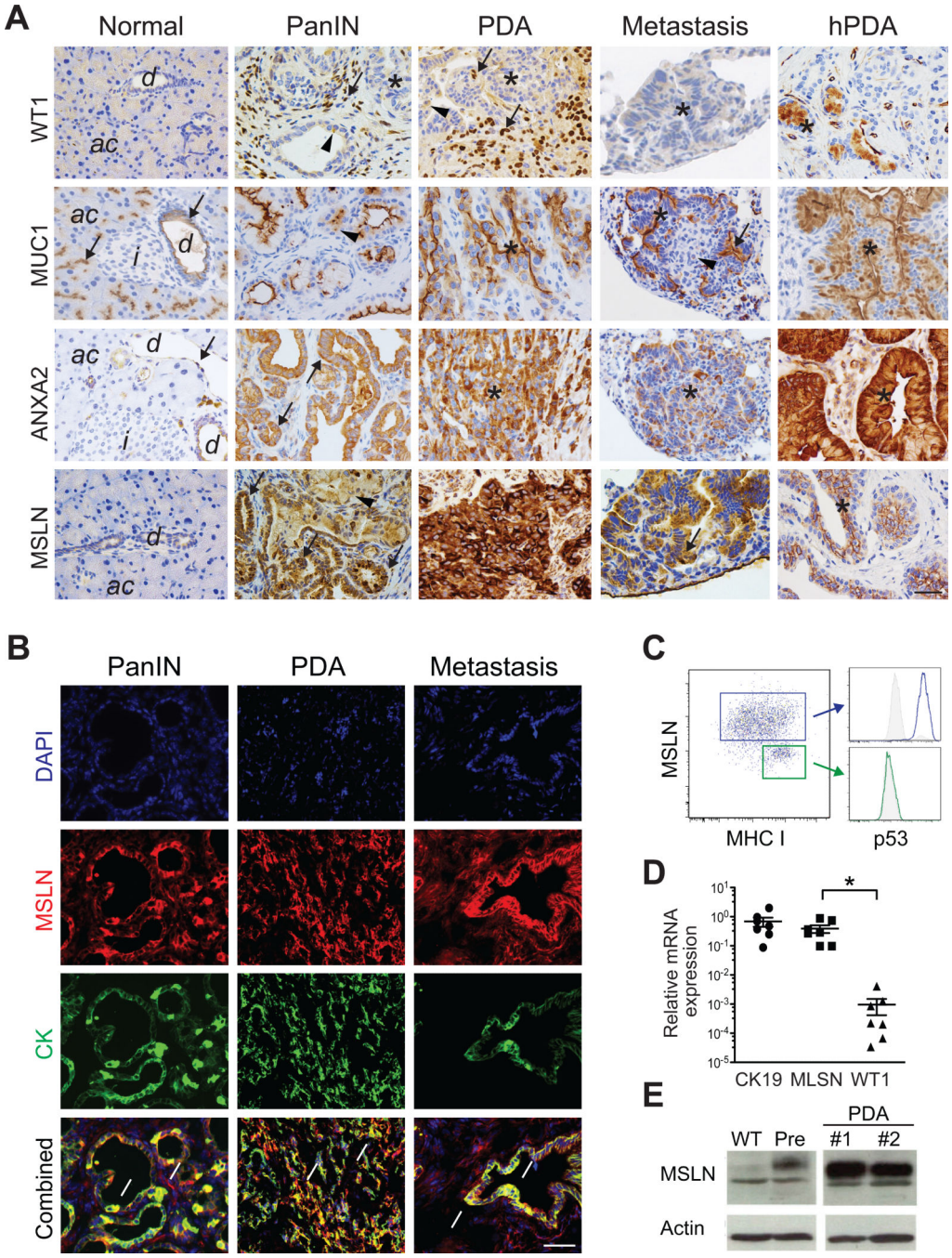

Figure 1. Tumor antigen expression in murine and human PDA

(A) Immunohistochemical analyses of target antigens in murine and human (hPDA) tissues. *d*, duct; *ac*, acini; *i*, islets; arrows, high expression; arrowheads, low-moderate expression; *, tumor epithelial cells. Scale bar, 25 μm.

(B) Immunofluorescence for MSLN and cytokeratin (CK) in indicated *KPC* tissues. Arrows, $MSLN^{+}CK^{+}$ cells. Scale bar, 25 μm.

(C) FACs plot of MSLN, MHC I and p53 in early passage (<3X) primary *KPC* PDA cells.

(D) Relative expression of indicated mRNAs in primary *KPC* PDA cells. Each point represents an independent cell preparation. Mean ± SEM.
(E) Immunoblot analyses of primary murine pancreatic ductal cells, primary preinvasive *KC* cells (Pre) and two independent invasive *KPC* PDA primary cell preparations.
See also Figure S1.

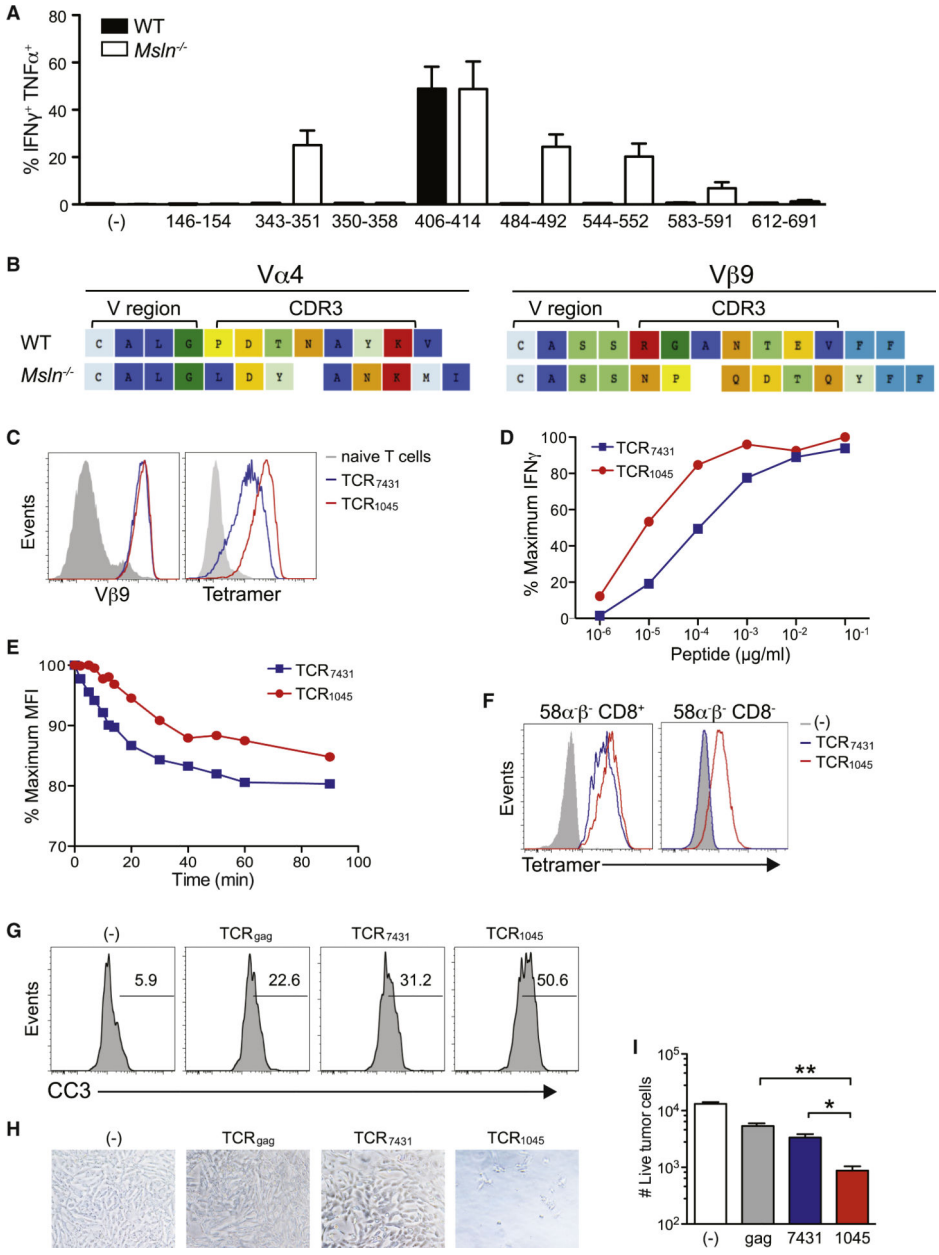

Figure 2. Cloning and expression of the enhanced-affinity TCR_{1045} $MSLN_{406-414}$-specific TCR

(A) Epitope mapping of MSLN-specific T cells derived from WT and $MSLN^{-/-}$ mice.

(B) CDR3 sequences of Vα4 and Vβ9 chains cloned from the highest avidity $MSLN_{406-414}$-specific T cell clones isolated from WT and $MSLN^{-/-}$ mice.

(C) Expression of $MSLN_{406-414}$-specific TCR derived from WT (TCR_{7431}) or $MSLN^{-/-}$ (TCR_{1045}) mice in P14 T cells after 2 *in vitro* stimulations.

(D) Functional avidity of engineered T cells assessed by intracellular IFNγ (normalized to maximum response).

(E) Dissociation kinetics of tetramer binding.

(F) Tetramer binding by $58\alpha^{-}\beta^{-}$ cells expressing TCR_{7431} or TCR_{1045} with or without CD8 co-receptor.

(G) Apoptosis of MHC class I^+ *KPC* tumor cells following incubation with engineered T cells.

(H) Residual adherent tumor cells following incubation (5 hr) with specified T cells.

(I) Number of live adherent tumor cells in (H) (assessed by trypan blue exclusion).

Data are shown as mean ± SEM. See also Figure S2.

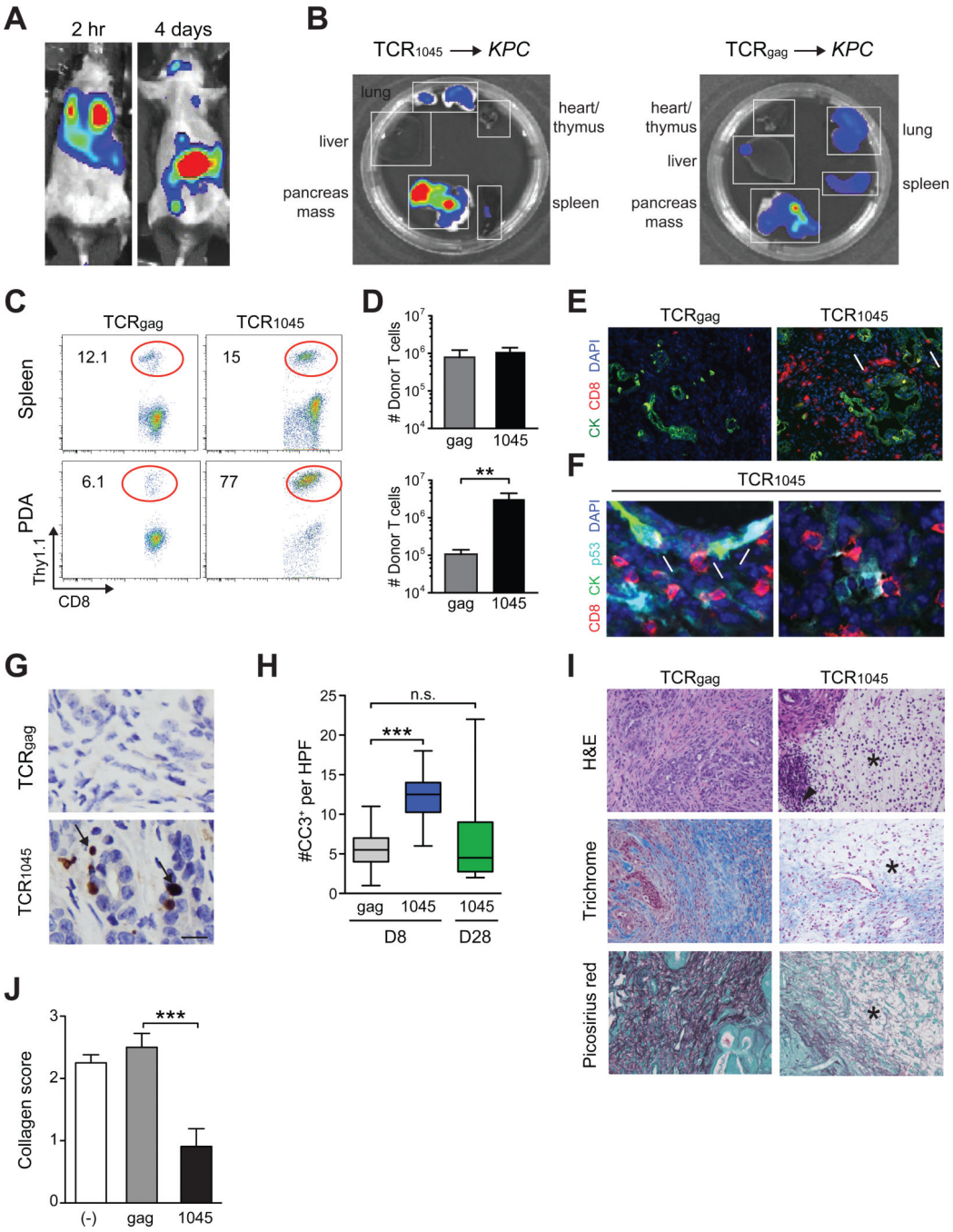

Figure 3. Biodistribution and *in vivo* effects of genetically engineered TCR_{1045} T cells

(A) Biodistribution of TCR_{1045} T cells 2 hr and 4 days post transfer into *KPC* mouse.

(B) Distribution of donor TCR_{1045} or TCR_{gag} cells in tissues *ex vivo* 8 days post transfer.

(C) Donor T cell frequency 8 days post transfer. Plots are gated on $CD45^+CD8^+$ cells.

(D) Number of donor T cells isolated from spleen (top) and tumor (bottom) 8 days post transfer.

(E) Immunofluorescence for CD8 and CK in primary tumors 8 days post transfer. Scale bar, 50 μm; arrows, CD8 T cells adjacent to epithelium.

(F) Immunofluorescence for indicated molecules in primary tumors 8 days post TCR_{1045} cell transfer. Arrows, CD8 T cells adjacent to $p53^{+}CK19^{+}$ tumor cells; arrowheads, $p53^{+}CK19^{-}$ cells in the stroma. Scale bar, 10 μm.

(G) IHC for cleaved-caspase 3 (CC3) in PDA at day 8. Arrows, $CC3^{+}$ cells. Scale bar, 10 μm.

(H) Tumor apoptosis 8 and 28 days post T cell transfer.

(I) Histology of pancreatic tumors 8 days post T cell transfer. *, absence of interstitial pink (H&E), blue (Masson's trichrome) and red (Picosirius) stain reflects a loss in ECM collagen content. Arrowhead, infiltrating mononuclear cells. Scale bar, 50 μm.

(J) Quantification of collagen content in tumors from (I).

Data are shown as mean ± SEM. See also Figure S3.

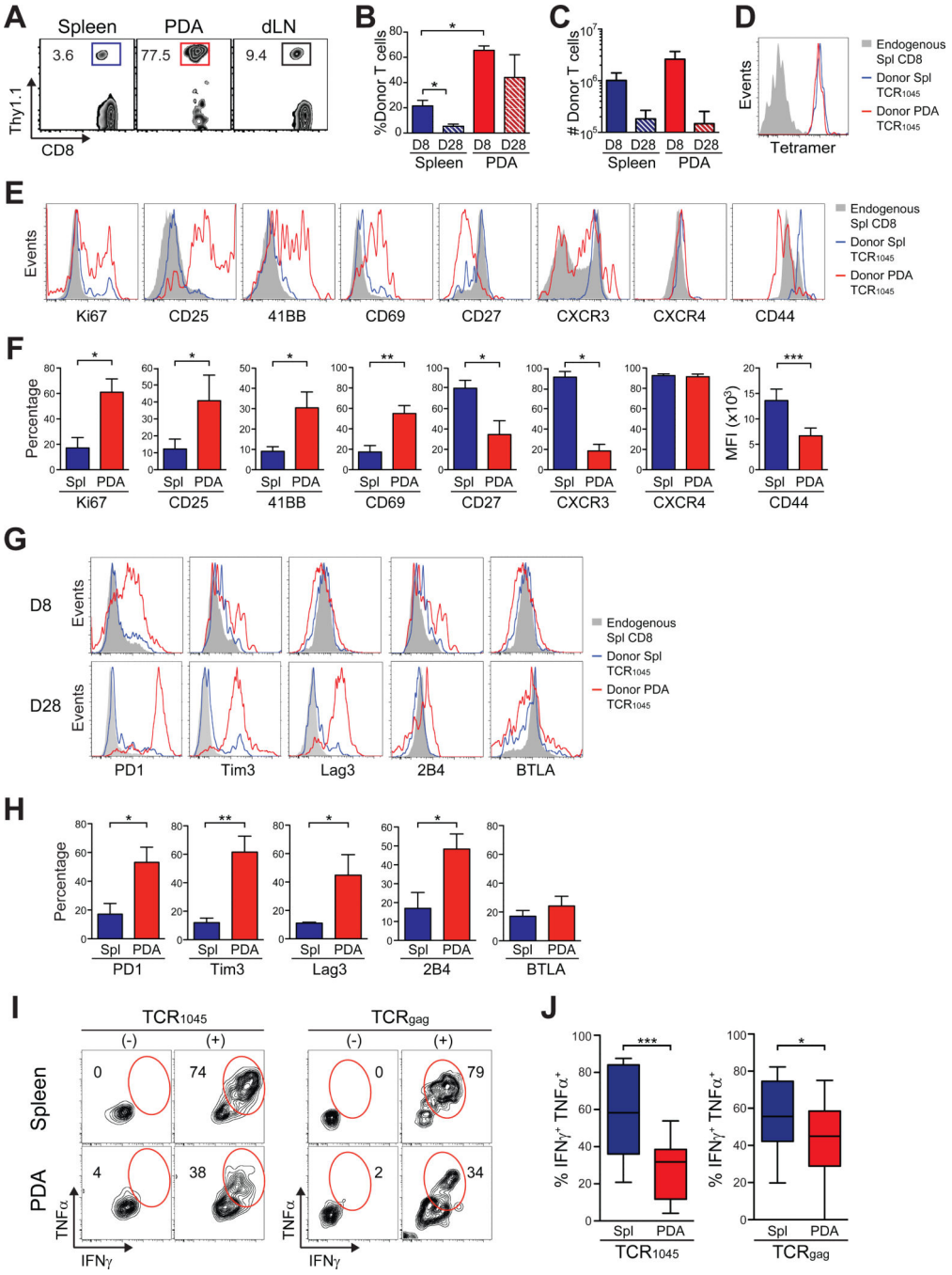

Figure 4. Tumor-infiltrating TCR_{1045} T cells have a phenotypic signature consistent with antigen recognition and are dysfunctional

(A) Donor TCR_{1045} cell frequency 28 days post T cell transfer. Plots are gated on $CD45^+CD8^+$ T cells.

(B) Donor TCR_{1045} cell frequency in spleens (Spl) and tumors 8 (D8) or 28 (D28) days post T cell transfer.

(C) Number of donor TCR_{1045} cells 8 or 28 days post T cell transfer..

(D) Tetramer staining of splenic and intratumoral donor TCR_{1045} cells 28 days post transfer.

(E) Phenotype of donor ($CD8^+Thy1.1^+$) TCR_{1045} cells compared to concurrently isolated splenic host ($CD8^+Thy1.1^-$) T cells 28 days post transfer.
(F) Frequency or MFI of donor T cells positive for indicated antigens in spleen and PDA. Mean ± SEM, n=3 each.
(G) Inhibitory receptor expression by donor TCR_{1045} cells and endogenous T cells.
(H) Frequency of donor TCR_{1045} cells expressing indicated molecules 28 days post T cell transfer.
(I) *Ex vivo* cytokine production by T cells in presence (+) or absence (−) of antigen 8 days post T cell transfer.
(J) Donor T cell frequencies producing both IFNγ and TNFα after 5 hr restimulation with antigen.
Data are shown as mean ± SEM. See also Figure S4.

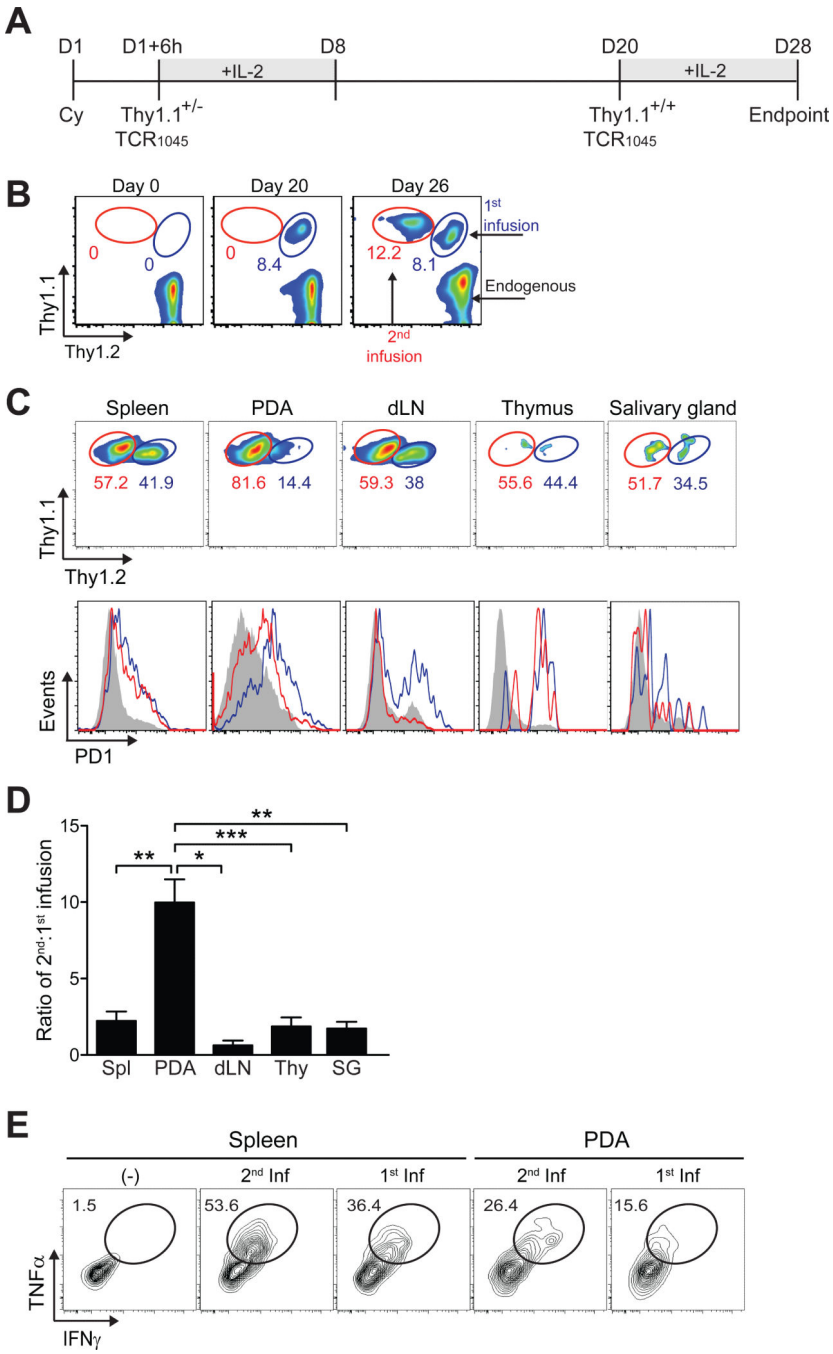

Figure 5. A second infusion of engineered TCR_{1045} cells also preferentially accumulates in PDA

(A) Schematic of congenically distinct T cell infusions into same *KPC* recipients. Cyclophosphamide (Cy) was administered prior to the 1st infusion only.

(B) Circulating CD8 T cells prior to transfer (D0), 20 days following first infusion of TCR_{1045} $Thy1.1^{+/-}$ cells (D20), and 6 days following second infusion of TCR_{1045} $Thy1.1^{+/+}$ cells (D26).

(C) Preferential accumulation and phenotype of second TCR_{1045} infusion in PDA (gated on $CD8^+Thy1.1^+$ cells). Concurrent PD1 expression on donor T cells from first (blue lines) and second (red lines) infusions. Grey histograms represent endogenous $CD8^+Thy1.1^-$ T cells.
(D) Ratio of persisting cells 8 days after second infusion. dLN, draining lymph node; Thy, thymus; SG, salivary gland.
(E) Cytokine production by donor T cells at day 28 (see (A)). Cells were stimulated together and plots gated on $CD8^+$ $Thy1.1^{+/-}$ (1st infusion) or $CD8^+$ $Thy1.1^{+/+}$ cells (2^{nd} infusion). Data are shown as mean ± SEM.

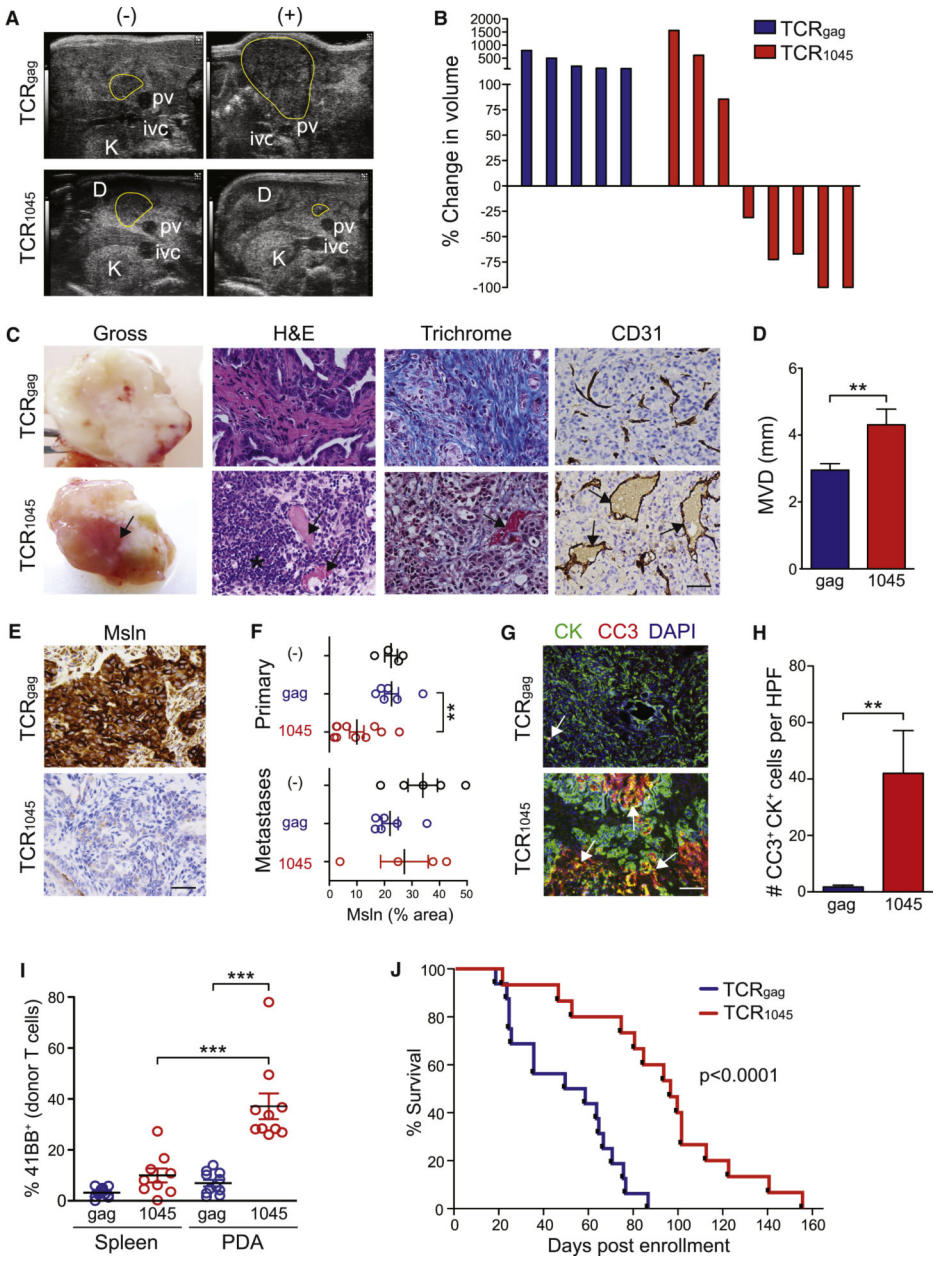

Figure 6. Serial infusions of engineered TCR_{1045} T cells significantly prolongs survival of *KPC* mice with established PDA

(A) High-resolution ultrasound images of pancreatic head mass before (−) and after (+) TCR_{gag} or TCR_{1045} cell therapy. D, duodenum; pv, portal vein; K, kidney; ivc, inferior vena cava.

(B) Waterfall plots of best observed response by serial imaging (results confirmed by two investigators).

(C) Gross and immunohistochemical analyses of PDA following T cell therapy. Arrows, blood flow and patent blood vessels; *, mononuclear cell infiltrate; scale bar, 25 μm.

(D) Mean vessel diameter (MVD) in PDA.

(E) MSLN expression in PDA following serial T cell infusions. Scale bar, 25 μm.

(F) MSLN staining intensity in primary tumors and metastases following T cell therapy. Each dot represents a primary tumor or metastasis.
(G) Dual immunofluorescence for apoptosis (CC3) in PDA epithelial cells (CK) following T cell therapy. Arrows, CK^+CC3^+ cells. Scale bar, 50 μm.
(H) Quantification of data in (G).
(I) Expression of 41BB by donor TCR_{gag} and TCR_{1045} cells. Points represent individual animals.
(J) Survival of *KPC* mice with invasive disease that received serial TCR_{gag} (n=16) or TCR_{1045} (n=15) T cell therapy (54 days vs 96 days, respectively; $p<0.0001$).
Data are shown as mean ± SEM. See also Figure S5 and Table S1.

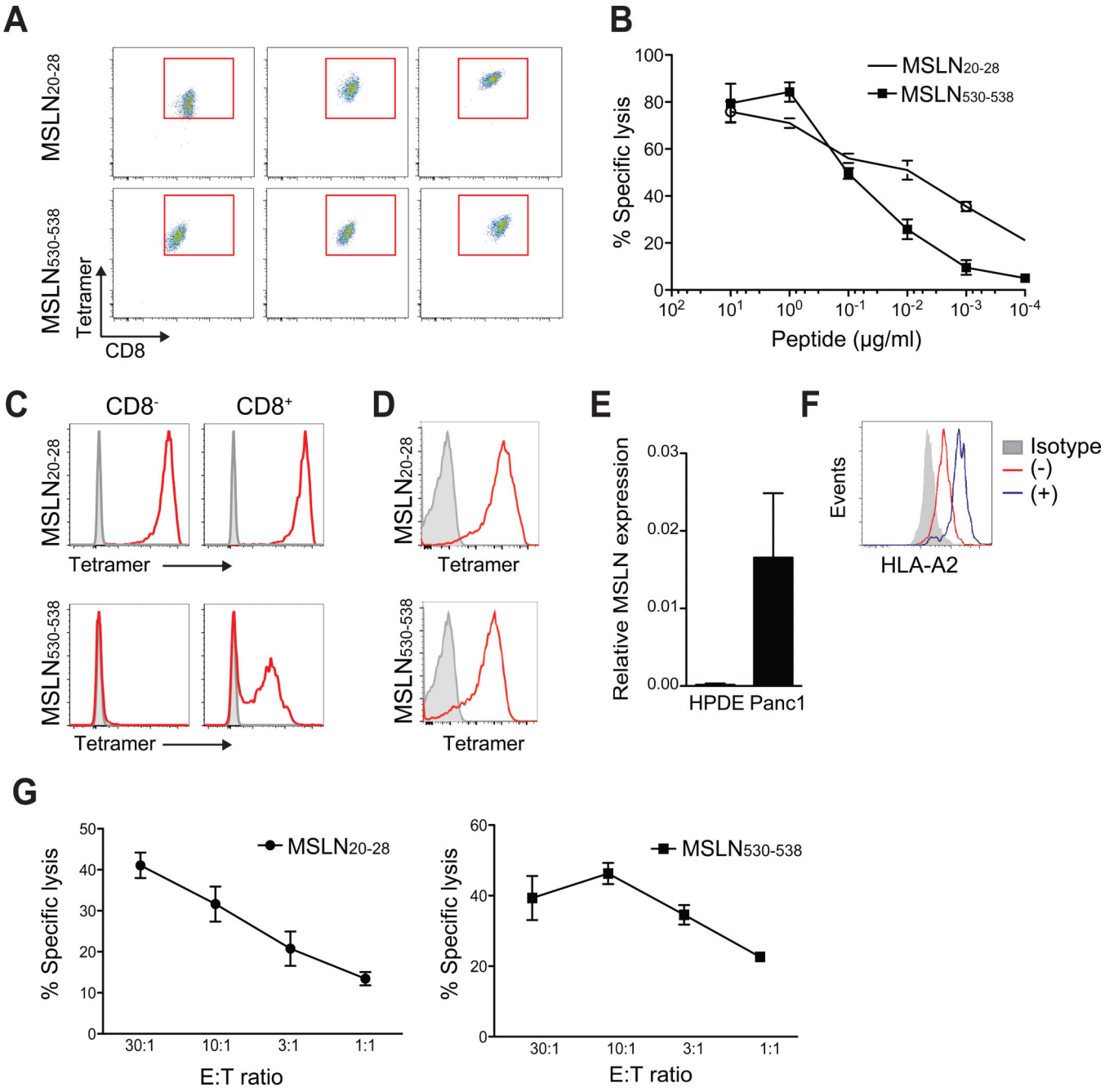

Figure 7. Isolation, expression and characterization of cloned human TCR specific to MSLN epitopes

(A) Tetramer staining intensities of independently derived HLA-A2-restricted human T cell clones with the indicated specificities. Representative of 10-12 clones analyzed per epitope.

(B) $MSLN_{20-28}$ and $MSLN_{530-538}$-specific T cell clone lysis of HLA-$A2^+$ T2 target cells loaded with titrating concentrations of peptide.

(C) Tetramer staining of $CD8^-$ and $CD8^+$ Jurkat cells transduced with $MSLN_{20-28}$- or $MSLN_{530-538}$-specific TCR.

(D) Tetramer staining of primary human CD8 T cells transduced with highest affinity $MSLN_{20-28}$ or $MSLN_{530-538}$-specific TCR.
(E) MSLN expression in human pancreatic ductal epithelial (HPDE) and Panc-1 cell lines (normalized to GAPDH).
(F) HLA-A2 expression by Panc-1 cells in the presence (+) or absence (−) of IFNγ.
(G) Lysis of HLA-$A2^+MSLN^+$ Panc-1 cell line by human CD8 effector T cell clones at indicated effector:target (E:T) ratios.
Data are shown as mean ± SD. See also Table S2.